Pakistan J. Zool., vol. 55(3), pp 1365-1371, 2023 DOI: https://dx.doi.org/10.17582/journal.pjz/20201106061108

Rivaroxaban Reduces Cerebral Hemorrhage in Mice with TPA Ischemic Stroke after Thrombolysis by Down-Regulating PAR-1 and PAR-2

Sen Ye[1], Jiangang Pang[2] and Xiuli Wang[3]*

[1]*Medical Records Department, Jinan Central Hospital, 250013, China*
[2]*Medical Imaging Department, Yidu Ce ntral Hospital of Weifang, Weifang, 252500, China*
[3]*General Practice of Kuangshan Community Service Center, Jinan Ind People's Hospital, Jinan, 250001, China*

Article Information
Received 06 November 2020
Revised 11 October 2020
Accepted 04 December 2020
Available online 30 June 2022 (early access)
Published 14 April 2023

Authors' Contribution
SY collected the samples. JP analysed the data. XW conducted the experiments and analysed the results. All authors discussed the results and wrote the manuscript.

Key words
Tissue plasminogen activator, Rivaroxaban, Cerebral hemorrhage (CLC Number) R657.4+4 (Document Identification Code) A

ABSTRACT

The objective of this study was to investigate the mechanism by which rivaroxaban reduces cerebral hemorrhage in mice with TPA ischemic stroke after thrombolysis. Male Wistar mice (11-week-old) as our experimental subjects were administered with warfarin (0.2 mg/kg/day), rivaroxaban (60 mg/kg/day), rivaroxaban (120 mg/kg) /day), or solvent pretreatment for 14 d to induce transient middle cerebral artery occlusion for 90 min, followed by perfusion with tPA (10 mg/kg/10ml). Infarct volume, bleeding volume, immunoglobulin G leakage and blood parameters were examined. PAR immunohistochemistry was performed on brain sections after 24 h reperfusion. We found that compared with the rivaroxaban group, the warfarin pretreatment group had an increased ICH volume; PAR-1, -2, -3, and -4 were widely expressed in the normal brain and there was higher expression in the ischemic brain, especially in ischemic peripheral lesions. Warfarin pretreatment enhanced the expression of PAR-1 and PAR-2 in preischemic and post-ischemic lesions, whereas rivaroxaban pretreatment had no such effect. This study suggests that rivaroxaban pretreatment causes lower risk of cerebral hemorrhage in mice than warfarin pretreatment. we conclude that, compared with warfarin pretreatment, the relative down-regulation of PAR-1 and PAR-2 in rivaroxaban pretreatment may be involved in the mechanism of reduction in bleeding complications.

INTRODUCTION

Atrial fibrillation increases with age, leading to cardioembolic stroke, a primary cause of stroke in the elderly (Douketis *et al*., 2016). Rivaroxaban is a highly selective oral drug (Linkins *et al*., 2016), which directly inhibits coagulation factor Xa, blocks the internal and external channels of the coagulation cascade, thus hindering thrombin generation and thrombosis (Bansilal *et al*., 2015). Tissue plasminogen activator (tPA), as a serine protease (Yousuf *et al*., 2016), plays a key role in the dynamic balance between coagulation and fibrinolysis (Baron *et al*., 2015). Studies have reported (Liu *et al*., 2015; Baron *et al*., 2015; Yousuf *et al*., 2016) that tPA can not only regulate physiological mechanism and neuroplasticity of the normal central nervous system, but also play an important role in pathological conditions (Piccolo *et al*., 2015). By increasing the amount and activity of matrix metalloproteinase-9 (MMP-9), tPA aggravates the damage of ischemic endothelial cells, and then worsens the destruction of blood-brain barrier (Alexandrov, 2015). The destruction of the blood-brain barrier after cerebral stroke is one important cause of brain injury (Haley *et al*., 2016). It can allow blood-borne inflammatory factors and harmful components to penetrate into the brain parenchyma (Shi *et al*., 2018). By upward adjustment of endothelial cell adhesion molecules, it can make a large number of monocytes and peripheral blood leukocytes persist and accumulate in the vascular injury site (Ren *et al*., 2015). The migration of cells to the brain parenchyma through the blood-brain barrier further activates a series of inflammatory cascade reactions, producing a large number of inflammatory mediators, and exacerbating the development of neuroinflammatory reactions as well as vasogenic brain edema in the brain.

* Corresponding author: wangxiuli030516@126.com
0030-9923/2023/0003-1365 $ 9.00/0

MATERIALS AND METHODS

Male Wistar mice (11 weeks old, with body weight 240-260 g) were acclimated for 2 weeks in standard mouse cages under conventional laboratory conditions with a 12/12 h light-dark cycle, constant humidity and room temperature of 238°C. These animals were fed with rat chow. Water was randomly packed in bottles. One mouse had one cage cleaned with pulp cushion every week. All animal experiments follow the experimental protocol approved by the Animal Committee of the Graduate School of Medicine and Dentistry, Okayama University.

Experimental group and drug treatment

The mice were divided into four groups: solvent treatment group (0.5% sodium carboxymethyl cellulose; V1+tPA), warfarin pretreatment group (0.2mg/kg/d; W+V1+tPA), low-dose rivaroxaban pretreatment group (60mg/kg/d; R(L)+tPA), high-dose rivaroxaban pretreatment group (120mg/kg/d; R(H)+tPA Fig. 1). Behavioral testing, surgery, and immunohistochemical analysis research were performed. Since 11-week age, each drug was used for 2 weeks. Warfarin was taken orally once a day, and rivaroxaban was fed weekly. In the mice venous thromboembolism model and pharmacokinetic (PK) experiment of rivaroxaban, dose of each drug and the interval between the last drug intake and the induction of cerebral ischemia were measured to inhibit thrombosis by 70% (Fig. 2). In the pharmacokinetic (PK) experiment of rivaroxaban, 50 Wistar mice were randomly fed with alkaline pellet feed containing 600 or 1200ppm rivaroxaban for 3 weeks. Then, at 5 sunshine time points, 5 animals were anesthetized in groups, and 5 ml whole blood was taken from each animal (Fig. 2). We estimate that each animal has a body weight of 250 g and a daily food intake of 25 grams (containing 600 ppm or 1200 ppm rivaroxaban). A daily diet of 25 g per animal is equivalent to a daily dose of 60 or 120 mg rivaroxaban. We provided each animal (one cage for one mouse) with 25 g food per day and observed whether these animals have eaten all the served food. We confirmed that most animals eat 25 g food every day. At 1h after the last administration of warfarin, blood was drawn from the left femoral vein. The prothrombin time (PT), activated partial prothrombin time (aPTT) and thrombin-antithrombin complex (TAT) were measured. PT, aPTT and TAT in the solvent group and rivaroxaban group were measured simultaneously with the warfarin group.

Focal cerebral ischemia

After 2 weeks of pretreatment, the mice were anesthetized with a nitrous oxide/oxygen/isoflurane mixture (69%:30%:1%) inhalation mask. During the operation, use a heating pad to monitor body temperature and maintain it at 37±0.3°C. As mentioned earlier, the right middle cerebral artery (MCA) was blocked by inserting a 4-0 surgical nylon thread and a silicon coating into the common carotid artery. 90 min after transient middle cerebral artery occlusion (tMCAO), the nylon thread was taken out gently to restore the blood flow in the MCA area, and the mice were treated with tPA (Grtpa) (intravenous injection, 10mg/kg/10ml). This relatively high dose of tPA was selected based on reports of a 10-fold difference in fibrin-specific activity between humans and rodents. To detect the bilateral 5% significance level and 80% power increase in ICH, a sample size of 30 mice per group is necessary if we assume that the expected withdrawal rate is 50%. We used 121 mice in this study, 66 of which were excluded based on the following criteria: Mice died of a procedural problem during surgery (n = 36), mice had no neurological outcome (n = 21), and mice died from the previous period (n = 9).

Tissue preparation

At 24 h after reperfusion, the surviving mice (total n = 55; 14 in V+tPA group, 13 in W+tPA group, 15 in R (L) + tPA group, 13 in R (H) + tPA group) were intraperitoneally injected with pentobarbital (40mg/kg) after anesthesia and perfused with ice-cold phosphate (PBS), followed by perfusion of ice-cold 4% paraformaldehyde phosphate buffer. The whole brain was taken out and immersed in the same fixing agent for 12h at a temperature of 4°C. After washing with PBS, the tissues were sequentially transferred to 10%, 20%, and 30% (w/vo) sucrose solutions, buried in dry ice powder, and stored at -80°C. The 20 μm thick sections were cut with a -80°C cryostat, and mounted on a silane-coated glass slide.

Histology and single immunohistochemical analysis

The brain section was observed under light microscope after hematoxylin-eosin staining to determine the ischemic injury area. 2, 0, 22, 24 and 26mm sections were cut from the bregma. The pixels of these 5 sections were counted with Photoshop CC, the infarct area was measured and the infarct volume was calculated by multiplying the infarct area by the thickness of 2 mm. For cerebral hemorrhage analysis, iron staining was done with enhanced Perl reaction. The sections were incubated with Perl solution (5% potassium ferrocyanide and 5% hydrochloric acid, 1:1) for 45 min, washed with distilled water, and re-incubated for 60 min with 0.5% diaminobenzidine tetrahydrochloride and nickel. To estimate mice IgG levels, sections were incubated with biotin-labeled rabbit anti-rat IgG antibody. Immune reaction was carried out in the horseradish peroxidase streptavidin-biotin complex solution, followed by incubation with diaminobenzidine hydrochloride. For further immunohistochemistry, we

adopted the following main antibodies: mouse anti-PAR-1 antibody (1:50;), mouse anti-PAR-2 antibody (1:50), goat anti-PAR-3 antibody (1:50), goat anti-PAR-4 antibody (1:50), rabbit anti-neuronal nuclear (NeuN) antibody (1:500), biotinylated pulsatilla lectin (LEL) (1:200), rabbit anti-glutathione S-transferase pi-1 (GST-p) antibody (1:500), rabbit anti-glial fibrillary acidic protein (GFAP) antibody (1:1000), rabbit anti-ionized calcium binding adapter molecule-1 (Iba-1) antibody (1:1000). LEL is a glycoprotein with affinity for n-acetylglucosamine oligomer (NAGO), which is expressed by mature vascular endothelial cells. To estimate the expression levels of PAR1, PAR2, PAR3 and PAR4, the sections were incubated with the corresponding primary antibody and then with the appropriate biotin-labeled secondary antibody (1:500).

Double immunofluorescence analysis

To determine the location of PAR in ischemic peripheral lesions, PAR-1, PAR-2, PAR-3 and PAR-4 were subject to double immunofluorescence study with NeuN, NAGO, GST-p, GFAP and Iba-1, respectively. Use appropriate fluorescent secondary antibodies, namely donkey anti-goat IgG antibody coupled to Alexa 555, to observe the immune response. Goat anti-mouse IgG antibody was coupled to Alexa 555, donkey anti-rabbit IgG antibody was coupled to Alexa 488, and chicken anti-rabbit IgG antibody was coupled to fluorescein isothiocyanate (FITC), fluorescein FITC antibody. The treated section was scanned and captured under argon and HeNe1 laser confocal microscope at 3100 times magnification.

Semi-quantitative analysis

For semi-quantitative evaluation of mice immunoglobulin and PAR (PAR-1, 2, 3, 4) staining intensity, the staining part of the caudate nucleus (1.2, 0.7 and 0.2mm lateral bregma) was selected randomly from cortical endodermis and lateral cortex of each mouse and the three areas on the same side of the body, and captured with optical microscope at 3200 times magnification. Staining intensity was measured with image processing software.

Data processing

The data was analyzed using SPSS v.22.0 (IBM, Armonk, NY). All data are expressed as mean ± SE. The between-subject analysis of variance was used to identify the difference in the lesions and the contralateral hemisphere before and after ischemia. One-way analysis of variance was taken to compare the four groups (V+tPA, W+tPA, R(L)+tPA, R(H)+tPA), and the Tukey honest significance test was performed on normally distributed data. Kruskal-Wallis analysis of variance test and Ryancorrected Mann-Whitney U test were performed to evaluate non-normally distributed data. P <0.05 indicates statistically significant difference.

RESULTS

Infarct volume, cerebral hemorrhage volume and IgG staining are strong

The 24-h survival rates after surgery in the V+tPA group, W+tPA group, R(L)+tPA group, and R(H)+tPA group are 93.3% (n=14), 76.5% (n=13), 88.2% (n=15), 86.7% (n=13), respectively, showing no significant difference (P>0.05). No difference is observed in infarct volume among the four groups (P>0.05), with results shown in Table I. However, compared with R(L)+tPA group and R(H)+tPA group, W+tPA group has greater ICH (Fig. 1). This difference is quantified and confirmed as shown in Table II. W+tPA group has significantly larger ICH volume than V+tPA group, R(L)+tPA group and R(H)+tPA group (Table II). W+tPA group has stronger IgG staining in neurons and nerve fibers, but the difference is insignificant between the four groups (P>0.05) (Fig. 2, Table II).

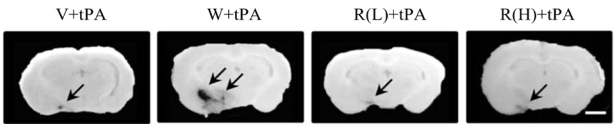

Fig. 1. Representative photographs of intracerebral hemorrhage (ICH) show: W+tPA group has stronger intracerebral hemorrhage (arrow), R(L)+tPA group has weaker intracerebral hemorrhage, (R(H)+tPA group has stronger intracerebral hemorrhage (arrow), R(L)+tPA has weaker intracerebral hemorrhage, (R)+tPA group has stronger intracerebral hemorrhage (arrow), and R(H)+tPA group has weaker intracerebral hemorrhage (arrow). Scale: 2mm.
For details of groups, see Table I.

Table I. Survival rate and infarct volume.

Group	V+tPA group	W+tPA group	R(L)+tPA group	R(H)+tPA	
Survival rate %	93.37±10.25	76.51±8.91	88.22±6.82	86.73±7.91	0.298
Infarct volume (mm^3)	175.72±8.33	172.51±10.25	170.3±7.62	176.32±8.31	0.352

V1+tPA, 0.5% sodium carboxymethyl cellulose; W+V1+tPA, warfarin pretreatment group (0.2mg/kg/d); R(L)+tPA, low-dose rivaroxaban pretreatment group (60mg/kg/d); R(H)+tPA, high-dose rivaroxaban pretreatment group (120mg/kg/d).

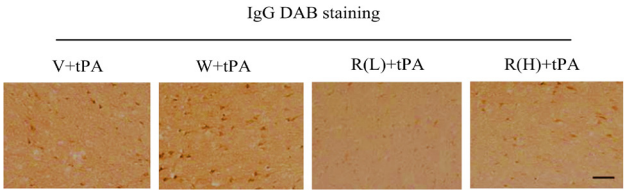

Fig. 2. W+tPA group has stronger IgG staining in neurons and nerve fiber network, but the difference is insignificant between the four groups. Scale: 50mm. For details of groups, see Figure 1 and Table I.

Table II. Quantification of intracerebral hemorrhage volume (ICH) and pixel intensity of IgG.

Group	Cerebral hemorrhage volume (mm^3)	Intensity
V+PA group	0.32±0.02	0.96±0.12
W+tPA group	1.89±0.12	1.39±0.51
R(L)+tPA group	0.28±0.03	0.58±0.11
R(H)+tPA	0.31±0.04	0.78±0.11

For details of groups, see Table I.

Blood analysis

Before tMCAO, compared with V+tPA group, W+tPA group, R(L)+tPA group and R(H)+tPA group have significantly prolonged prothrombin time (PT) (P<0.05). No significant difference is shown in activated PT (aPTT) among the four groups. Compared with V+tPA group, W+tPA group, R(L)+tPA group, and R(H)+tPA group have significantly lower TAT, but there is no difference between W+tPA group, R(L)+tPA group, and R(H)+tPA group. This result supports that the three drug groups have the same anticoagulation level (Table III).

Immunoreactivity of PAR 1-4

PAR-1, PAR-2, PAR-3 and PAR-4 are widespread but weakly expressed in normal brains. Evaluated by pixel intensity, their levels increase in the ischemic brain, especially in the ischemic peripheral lesions. Immune response of PAR-1 and PAR-2 was mainly detected in neurons in the V+tPA group, but weaker in the blood vessels of ischemic lesions. PAR-3 immunoreactivity was found in both neurons and blood vessels, while PAR-4 was only observed in neurons. Compared with V+tPA group, W+tPA group had significantly increased number and pixel intensity of PAR-1 in the periphery of the ischemic lesion (P<0.05), while no such increase was found in low-dose rivaroxaban group. Similar to PAR-1, pixel intensity increase of PAR-2 in ischemic lesion W+tPA group (P<0.05) was not observed in low-dose rivaroxaban treatment. In addition, R(L)+tPA group had lower PAR-2 pixel intensity in the contralateral hemisphere compared with W+tPA group (P<0.05). Compared with W+tPA group, R(L)+tPA group and R(H)+tPA group had reduced number of PAR-3 positive cells in the contralateral hemisphere (P<0.05). However, there was no significant difference in lesions before and after ischemia (P>0.05). Also, no significant difference was found in the number and density of PAR-4 pixels in the contralateral cerebral hemisphere before and after ischemia (P>0.05) (Table V).

PAR 1-4 double immunostaining of ischemic peripheral lesion

The double immunofluorescence study of V+tPA group showed that PAR-1 co-domain with some new neurons. PAR-1 usually does not co-localize with NAGO-positive vascular endothelial cells, but a small amount of PAR-1 immunoreactive activity is localized near endothelial cells. On the other hand, PAR-1 did not co-localize with GST-positive oligodendrocytes, GFAP-positive astrocytes, or Iba-1-positive microglia. PAR-2 also co-domains with some neurons and is distributed adjacent to a few endothelial cells. Similar to PAR-1, PAR-2 does not co-localize with oligodendrocytes, astrocytes or microglia. Unlike PAR-1 and PAR-2, PAR3 features strong co-domain with neurons and vascular endothelial cells, but not with oligodendrocytes, astrocytes or microglia. PAR-4 only co-domains with some neurons, but not with vascular endothelial cells, oligodendrocytes, astrocytes or microglia.

Table III. Blood analysis results.

Group	V+tPA group	W+tPA group	R(L)+tPA group	R(H)+tPA	P
Prothrombin time PT(s)	8.41±0.59	10.24±0.60	8.05±0.81	9.18±0.35	0.001
activated partial thromboplastin time aPT(s)	27.37±0.36	28.14±0.81	29.22±0.51	30.39±0.82	0.001
Thrombin-antithrombin complex (ng/mL)	7.68±0.51	4.25±0.36	3.92±0.32	3.56±0.11	0.001

For details of groups, see Table I.

Table IV. Number and pixel intensity of protease-actived receptors (PARs) staining in lateral hemisphere, ischemic injury (PAR-2, 3, 4) area, and contralateral hemisphere (PAR-2, 3, 4) different parts of brain.

Group	Number	Intensity
PAR-1 staining		
V+tPA group	38.41±6.28	1.23±0.11
W+tPA group	66.20±8.15	2.65±0.23
R(L)+tPA group	34.45±6.12	1.04±0.11
R(H)+tPA	42.62±4.95	1.81±0.16
P	0.001	0.001
PAR-2 staining		
V+tPA group	15.62±3.05	3.24±0.41
W+tPA group	38.24±5.16	14.56±2.32
R(L)+tPA group	18.68±1.53	6.26±1.11
R(H)+tPA	36.60±2.12	10.58±2.42
	0.001	0.001
PAR-3 staining		
V+tPA group	52.31±8.9	2.67±0.12
W+tPA group	53.15±6.1	2.72±0.33
R(L)+tPA group	48.62±6.5	2.07±0.21
R(H)+tPA	49.82±4.3	2.51±0.16
	0.102	0.211
PAR-4 staining		
V+tPA group	37.33±2.62	7.27±0.13
W+tPA group	33.10±1.1	7.32±0.32
R(L)+tPA group	32.62±1.4	8.30±0.56
R(H)+tPA	36.81±2.3	10.16±1.23
	0.153	0.125

For details of groups, see Table I.

DISCUSSION

PAR-1 is widely expressed in the brain, reaching neurons, vascular endothelial cells, oligodendrocytes, astrocytes and microglia (Huang *et al*., 2015). However, in this study, double staining showed that PAR-1 mainly localizes in neurons, with low content in vascular endothelial cells, but does not co-domain with GST-p (oligodendrocytes), GFAP (astrocytes) or Iba-1 (microglia) (Driesbaugh *et al*., 2015). PAR-1 agonists increase the cerebral infarction volume after cerebral ischemia, trigger astrocyte proliferation, activate microglia, and increase mRNA expression in IL-6, IL-1b and TNF-a, while there is no such phenomenon in mice lacking PAR-1 (Yi *et al*., 2010; Shimizu *et al*., 2017). In this study, warfarin pretreatment enhanced the expression of PAR-1 in ischemic peripheral lesions. PAR-2 is also widely expressed in the brain *in vivo* (Caelers *et al*., 2015), reaching neurons, astrocytes and microglia, but its expression is only observed in vascular endothelial cells cultured *in vitro*. However, in the current study, we did observe the expression of PAR-2 in brain vascular endothelial cells of mice. It has been reported (Driesbaugh *et al*., 2015; Sales *et al*., 2015) that after cerebral ischemia in mice, PAR-2 expression increases, and gene deletion will increase infarct volume and brain damage. Judging from the expression level and cell type, PAR-2 has neuroprotective or neurodegenerative effects. In this study, we found that warfarin pretreatment enhanced the expression of PAR-2.

As a cofactor, PAR-3 participates in the expression of thrombin signal in mouse platelets, and promotes the fission and activation of PAR-4 (Morihara *et al*., 2016). Some reports have demonstrated that PAR-3 is distributed in the brain, reaching neurons, vascular endothelial cells, astrocytes and microglia (Chen *et al*., 2018). We observed the up-regulation of PAR-3 in mouse brain neurons and blood vessels after ischemia, suggesting that after cerebral ischemia, PAR-3 participates in the process of ischemic brain injury or repair through neuronal and vascular endothelial mechanisms. Under pathological conditions, PAR-4 is a key regulator of blood coagulation and inflammation. Mice lacking PAR-4 have reduced infarct volume, suggesting neurodegenerative effects and exacerbated inflammatory effect. Similar to previous reports, PAR-4 levels were elevated in the ischemic brain, but PAR-4 expression showed no difference between the two groups treated with warfarin and rivaroxaban.

Many reports believe that FXa impacts a variety of molecular effects by activating PAR-1 and PAR-2, and rivaroxaban can prevent FXa-induced PAR-1 and PAR-2 activity, thereby leading to reduced inflammation (Wang *et al*., 2018). In this study, the enhanced expression of PAR-1 and PAR-2 found in the warfarin group was largely not caused by rivaroxaban treatment. Rivaroxaban reduces MMP-9 activity, while NVU dissociation, cerebral hemorrhage and IgG leakage may be related to the inhibition of PAR-1 and PAR-2 activity.

CONCLUSION

This study suggests that compared with warfarin pretreatment, rivaroxaban pretreatment of mice decreases risk of cerebral hemorrhage after cerebral ischemia and tPA treatment. Warfarin-induced up-regulation of PAR-1 and PAR-2 was not observed in rivaroxaban pretreatment, suggesting that activated PAR-1 and PAR-2 may be related to brain damage, such as destruction of the blood-brain

barrier and cerebral hemorrhage after tPAg. In contrast, there was no difference in the expression levels of PAR-3 and PAR-4 in mice treated with warfarin and rivaroxaban. To conclude, rivaroxaban reduces cerebral hemorrhage, MMP-9 activity, NVU dissociation and IgG leakage in mice with TPA ischemic stroke after thrombolysis, which has relation to the inhibition of PAR-1 and PAR-2 activity.

Statement of conflict of interest

The authors have declared no conflict of interest.

REFERENCES

Alexandrov, A.V., 2015. Combined lysis of thrombus with ultrasound and systemic tissue plasminogen activator for emergent revascularization in acute ischemic stroke (CLOTBUST-ER): An update. *J. Acoustic. Soc. Am*., **138**: 1819-1826. https://doi.org/10.1121/1.4933772

Bansilal, S., Bloomgarden, Z., Halperin, J.L., 2015. Efficacy and safety of rivaroxaban in patients with diabetes and nonvalvular atrial fibrillation: The rivaroxaban once-daily, oral, direct factor xa inhibition compared with vitamin K antagonism for prevention of stroke and embolism trial in atrial fibril. *Am. Heart J*., **170**: 675-82.e8. https://doi.org/10.1016/j.ahj.2015.07.006

Baron, E.M., Burke, J.A., Akhtar, N., 2015. Spinal epidural hematoma associated with tissue plasminogen activator treatment of acute myocardial infarction. *Catheter. Cardiovasc. Interv*., **48**: 390-396. https://doi.org/10.1002/(SICI)1522-726X(199912)48:4<390::AID-CCD15>3.0.CO;2-M

Caelers, A., Schmid, A.C. and Hrusovsky, A., 2015. Insulin-like growth factor II mRNA is expressed in neurones of the brain of the bony fish Oreochromis mossambicus, the tilapia. *Eur. J. Neurosci*., **18**: 355-363. https://doi.org/10.1046/j.1460-9568.2003.02761.x

Chen, S., Chen, Z. and Cui, J., 2018. Early abrogation of gelatinase activity extends the time window for tpa thrombolysis after embolic focal cerebral ischemia in mice. *e Neuro*, **5**: 391-317. https://doi.org/10.1523/ENEURO.0391-17.2018

Douketis, J.D., Spyropoulos, A.C. and Kaatz S., 2016. Perioperative bridging anticoagulation in patients with atrial fibrillation. *J. Vascul. Surg*., **63**: 823. https://doi.org/10.1016/j.jvs.2015.11.010

Driesbaugh, K.H., Buzza, M.S. and Martin, E.W., 2015. Proteolytic activation of the protease-activated receptor (PAR)-2 by the GPI-anchored serine protease testisin. *J. biol. Chem*., **290**: 3529-3541. https://doi.org/10.1074/jbc.M114.628560

Haley, M.J. and Lawrence, C.B., 2016. The blood-brain barrier after stroke: Structural studies and the role of transcytotic vesicles. *J. Cereb. Blood Flow Metabol*., **37**: 0271678X16629976. https://doi.org/10.1177/0271678X16629976

Huang, Q.T., Chen, J.H. and Hang, L.L., 2015. Activation of PAR-1/NADPH oxidase/ros signaling pathways is crucial for the thrombin-induced sflt-1 production in extravillous trophoblasts: Possible involvement in the pathogenesis of preeclampsia. *Cell Physiol. Biochem.,* **35**: 1654-1662. https://doi.org/10.1159/000373979

Linkins, L.A., Warkentin, T.E. and Pai, M., 2016. Rivaroxaban for treatment of suspected or confirmed heparin-induced thrombocytopenia study. *Hematol/Oncol. Clin. N. Am*., **14**: 1206-1210. https://doi.org/10.1111/jth.13330

Liu, Z., Li, Y. and Zhang, L., 2015. Subacute intranasal administration of tissue plasminogen activator increases functional recovery and axonal remodeling after stroke in rats. *Neurobiol. Dis*., **45**: 804-809. https://doi.org/10.1016/j.nbd.2011.11.004

Morihara, R., Yamashita, T. and Kono, S., 2016. Reduction of intracerebral hemorrhage by rivaroxaban after tPA thrombolysis is associated with downregulation of PAR-1 and PAR-2. *J. Neurosci. Res*., **95**: 1818-1828. https://doi.org/10.1002/jnr.24013

Piccolo, F., Popowicz, N. and Wong, D., 2015. Intrapleural tissue plasminogen activator and deoxyribonuclease therapy for pleural infection. *J. Thorac. Dis*., **7**: 999.

Ren, A., Amaro, S. and Laredo, C., 2015. Relevance of blood-brain barrier disruption after endovascular treatment of ischemic stroke: dual-energy computed tomographic study. *Stroke*, **46**: 673-679. https://doi.org/10.1161/STROKEAHA.114.008147

Sales, K.U., Friis, S. and Konkel, J.E., 2015. Non-hematopoietic PAR-2 is essential for matriptase-driven pre-malignant progression and potentiation of ras-mediated squamous cell carcinogenesis, *Oncogene*, **34**: 346-356. https://doi.org/10.1038/onc.2013.563

Shi, J., Peng, H. and You, S., 2018. Increase in neutrophil after r-tpa thrombolysis predicts poor functional outcome of ischemic stroke: A longitudinal study. *Eur. J. Neurol.*, **25(Suppl. 2)**: 687-e45. https://doi.org/10.1111/ene.13575

Shimizu, S., Tojima, I. and Takezawa K., 2017. Thrombin and activated coagulation factor X

stimulate the release of cytokines and fibronectin from nasal polyp fibroblasts via protease-activated receptors. *Am. J. Rhinol. Allergy*, **31**: 13-18. https://doi.org/10.2500/ajra.2017.31.4400

Wang, P., Yan, D.M. and Huang, X., 2018. The neuroprotection molecular basis and mechanism of Panax Notoginseng saponins in the treatment of ischemic stroke. *Chin. pharmacol. Bull.,* **34**: 1750-1755. https://doi.org/10.3969/j.issn.1001-1978.2018.12.025

Yi, Z., Sun, J. and Yang, X.R., 2010. Effects of Xuelian injection on cerebral TNF-α, IL-1β and MMP-9 in rats experienced focal cerebral ischemia/reperfusion. *J. Apoplxy Nervous Dis*., **7**: 2632.

Yousuf, T., Brinton, T. and Ahmed, K., 2016. Tissue plasminogen activator use in cardiac arrest secondary to fulminant pulmonary embolism. *J. Clin. med. Res*., **8**: 190. https://doi.org/10.14740/jocmr2452w